Dynamics of Hybrid III-V Silicon Semiconductor Lasers for Integrated Photonics

Kevin Schires, Nils Girard, Ghaya Baili, Guang-Hua Duan, *Senior Member, IEEE*, Sandra Gomez, and Frédéric Grillot, *Senior Member, IEEE*

***Abstract*—The dynamics of hybrid III-V/Si lasers are studied for the first time under a combination of two optical feedbacks. A cleaved fiber placed about 20 μm away from the laser creates a short feedback cavity. The effect of this short feedback is studied on a Fabry–Perot laser and reveals the sensitivity of the device to such perturbation, as well as the presence of sub-cavities in the Si waveguides. The dynamics of the laser subjected to additional feedback from a 70-m fiber cavity show that the long-feedback dynamics are governed by the sub-cavities. This behavior is confirmed using a complex tunable III-V/Si laser.**

***Index Terms*—III-V materials, nonlinear dynamics, optical feedback, silicon photonics.**

I. Introduction

SILICON photonics have generated increasing interest in recent years in domains such as optical communications, optical signal processing and sensing. Indeed, requirements on data rates for communication systems and on integration for embedded systems keep increasing [1]. The integration of optical functions on a microelectronic chip thus brings many innovative perspectives, along with the possibility to enhance the performances of photonic and electronic circuits [2]. In this general context, numerous research works have shown promising solutions to meet those future needs and silicon photonics is now seen as the solution of choice for the next generations of high-frequency circuits. Indeed, the Si platform takes benefit of a mature technology first developed for microelectronics in a context of high volume production. Furthermore, the convergence between electronic and photonic circuits on a same chip will allow signal processing to be performed closer to the receiver and the emitter. This should lead to a drastic reduction of the circuit size and allow novel ways of handling and transmitting data, leading to a significant improvement of performances [3], [4].

Recent progress in III–V foundry processes has made possible photonic integrated circuits (PICs) applicable to a wide range of applications [5], [6]. The monolithic integration of both passive (isolators, circulators, couplers, etc.) and active components (active isolators, lasers, modulators, amplifiers and photo-detectors) with very high densities allows for complex circuits with a steadily increasing number of components [7]–[13].

Although recent works have reported substantial breakthroughs on the epitaxial growth of III-V layers on Si [14]–[16], practical Si-based light sources are still missing, hence research is currently strongly focused on heterogeneous integration of III-V semiconductors on Si through wafer bonding techniques [17]–[19]. As a consequence, the future of PICs currently relies on complex designs where light is coupled between III-V and Si waveguides, those devices being in addition destined to be monolithically integrated close to other optical components, all source of optical reflections. Such complex devices thus require careful study of their dynamical properties, in particular when a laser may be subjected to any external light fed back into the cavity [20].

Indeed, it is known that the performances of a semiconductor laser are strongly altered by any type of external optical feedback. Five distinct regimes based on spectral observation have been reported for semiconductor distributed feedback (DFB) laser cavities [21]. Laser sensitivity can be such that even under weak feedback of a few percent, a laser can become unstable and operate within complex dynamical regimes [22]. In the special case of integrated photonics, identifying the sensitivity to optical feedback of novel laser sources involves studying the impact of external cavities below a few centimeters to simulate reflections from nearby components, cavities a few meters long to simulate reflections from the short fiber network, but also finding sources of parasitic reflections inside the laser cavity, such as at the interface between the III-V material and the Si waveguide [23]. Up to now, little is known on the stability of such integrated lasers.

In addition, optical feedback should not only be seen as a detrimental phenomenon but also as a well-established technique to create, e.g., chaotic transmitter for secure transmissions [24], and any parasitic reflection may make it difficult to transpose such well-known techniques to silicon photonics. In [25], an integrated laser with a filtered-feedback configuration is studied. The dynamics of the laser under feedback were investigated as a function of the feedback phase and injection

Manuscript received February 07, 2016; revised April 18, 2016; accepted April 18, 2016. This work was supported by the French National Research Agency (ANR) through the Nanodesign Project funded by the IDEX Paris-Saclay, ANR-11-IDEX-0003-02.

K. Schires and S. Gomez are with the CNRS LTCI, Télécom ParisTech, Université Paris-Saclay, Paris 75643, France (e-mail: schires@telecom-paristech.fr; sandra.gomez@telecom-paristech.fr).

F. Grillot is with the CNRS LTCI, Télécom ParisTech, Université Paris-Saclay, Paris 75643, France, and also with the Center for High Technology Materials, University of New-Mexico, Albuquerque, NM 87131 USA (e-mail: grillot@telecom-paristech.fr).

N. Girard, G. Baili, and G. H. Duan are with the III-V Lab, a joint lab of Alcatel-Lucent Bell Labs France, Thales Research and Technology and CEA Leti, Campus Polytechnique, Palaiseau 91767, France (e-mail: nils.girard@3-5lab.fr; ghaya.baili@thalesgroup.com; guanghua.duan@3-5lab.fr).

Color versions of one or more of the figures in this paper are available online at http://ieeexplore.ieee.org.

Digital Object Identifier 10.1109/JSTQE.2016.2565462

current, revealing both stable single-frequency regimes and various unstable ones. More recently, an active–passive integrated coupled cavity laser was experimentally demonstrated [26]. The laser is made with an InGaAsP/InP multiple quantum well structure, monolithically integrated with transparent ridge waveguides. The coupling between the two cavities is tolerant against the power fluctuations of the cavities, and leads to a laser with a side mode rejection ratio of 40 dB combined with a tuning range of 6.5 nm via integrated phase sections. Another work has reported the very first experimental bifurcation scenario in a laser with short external cavity embedded in a PIC consisting of a DFB laser bounded to a photodiode and a 2.3 mm-long active external cavity [27]. The dynamical scenario consisted of cycles of stationary states, self-pulsations of increasing frequency, and quasi-periodicity induced by the increase of the feedback strength, pointing out the possibility to generate high-frequency harmonic optical oscillations without electrical modulation.

In this work, we go a step beyond by providing the very first experimental investigation of novel III-V hybrid silicon lasers subjected to optical feedback. Compared to recently reported devices directly grown on Si [28], these devices allow study of the dynamics of a III-V active region within a Si optical cavity. Practically, hybrid integration of III-V on Si also allows using CMOS-compatible processes to create the complex waveguides constituting the PIC without any constraints from the III-V growth, the active region being wafer-bonded later on. The devices are first presented in Section II. In Section III and IV, comprehensive experimental results are shown for a Fabry–Perot (FP) laser under a combination of two types of optical feedbacks: very short cavity free-space feedback and long-cavity fibered feedback. Results show that short-cavity feedback greatly impacts the behavior of the laser and influences the route to chaos under long-cavity feedback. The impact of sub-cavities in the Si waveguide is also discussed. In Section V, the dynamics of a tunable laser (TUL) based on an extension of the FP laser design is studied under long-cavity feedback only. Finally, we summarize our results and conclusions in the last section. Based on the experimental results reported here, researchers can make an informed judgment about the optimization to be done for the development of future high-speed integrated circuits.

II. Devices Studied and Experimental Setup

The devices under study are based on a FP laser cavity inspired from [10]. The fabrication starts with 200 mm SOI wafers with a 440 nm thick silicon top layer. The first step is the formation of silicon rib waveguides by etching 220 nm the silicon layer. These rib waveguides are optimized for the coupling with III-V waveguides that will be aligned on top of the silicon waveguides in a later step. After this etching step, the remaining silicon layer has a thickness of 220 nm. Subsequent etching steps are applied to form rib and strip waveguides and other elements such as Bragg reflectors or vertical output couplers. After those steps, a silica layer is deposited and a chemical-mechanical polishing is applied in order to achieve a very flat top surface for the silicon wafer. In the meantime, 2" InP wafers are grown. The III-V region consists of a p-InGaAs contact layer, a p-InP cladding layer, 6 InGaAsP quantum wells surrounded by two InGaAsP separate confinement heterostructure layers, and an n-InP layer. Then the InP wafers are bonded onto the SOI wafers. After wafer bonding and InP substrate removal, dry etching is used to etch through the InGaAs layer and partly etch the InP p-doped waveguide cladding layer. The InP etching is completed by chemical selective etching. The multi-quantum well layer is etched by CH4:H2 RIE. The active waveguide is finally encapsulated with DVS- benzocyclobutene. A Ti/Pt/Au alloy is used for metallization on both p and n sides. Finally, the fabricated lasers are ready to be tested on the wafer through the use of vertical grating couplers.

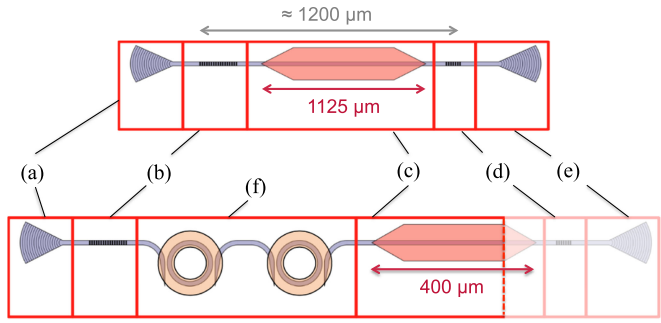

Fig. 1. Schematic views of the FP (top) and TUL (bottom) studied in this paper, with the Si waveguides shown in grey. The lettered sections correspond to (a) and (e) vertical couplers, (b) high-reflectivity DBR, (c) III-V gain section, (d) low-reflectivity DBR, and (f) Si rings. The doted red line on the TUL design shows where the samples used in this study were cleaved.

Fig. 1 presents diagrams of the structure of the two types of devices studied: a FP laser and a TUL. The main device is a FP laser consisting of a 1.2 mm-long optical cavity. The InP-based amplification section, sitting above the Si waveguide, occupies most of the cavity and each end is tapered to allow modal transfer between the III-V and Si waveguides. About 140 μm away from the tip of each tapers, distributed Bragg reflectors (DBRs) with reflectivities of 30% and 100%, form the optical cavity. Outside the cavity, additional Bragg gratings with reflectivities below 1% are placed about 130 μm away from the cavity's DBRs to allow vertical output fiber coupling [6].

The design of the TUL is more complex, with an active region only 400 μm-long and Si waveguides that include two ring resonators with metal heaters on top of the rings for thermal wavelength tuning. These have free spectral ranges (FSR) of 400 and 440 GHz, respectively, allowing selection of a single cavity mode if tuned appropriately, thus enabling tunable single-mode emission. As will be later discussed, the TULs studied in this work were cleaved in the III-V region, thus removing one of the tapers as well as the Si waveguide containing the cavity's lower-reflectivity mirror and the vertical coupler. The motivation to study these complex structures in addition to the FP lasers was to both confirm the results obtained with the latter but also to study an actual device used as TUL source for practical applications.

Fig. 2 presents a schematic of the experimental fiber setup used for characterization of the free-running laser as well as optical feedback experiments. Two external cavities can be

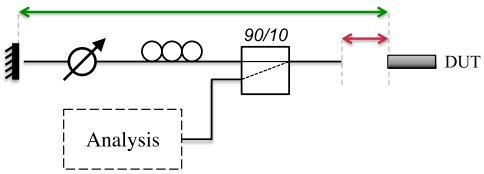

Fig. 2. Experimental setup used in this study. The red and green arrows show the short and long external cavities, respectively. The analysis part consisted either in combinations of a power-meter and optical and electrical spectrum analyzers. DUT: device under study.

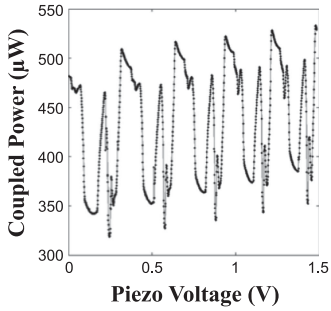

Fig. 3. Evolution of the coupled light with the voltage applied to the piezoelectric actuator displacing the fiber along the vertical axis.

considered. First, a short free-space cavity (red arrow on the schematic) of the order of 20 μm can be created by the tip of the fiber, used to both collect the light emitted by the device under test (DUT) and inject the light from the longer cavity. The latter is a fiber cavity (green arrow on the schematic) about 7 m long, created using a Yenista back-reflector module equivalent to a mirror with adjustable losses, as depicted on the experimental diagram. While the back-reflector preserves the light's polarization over its whole range of attenuation, it is unclear whether the phase changes as the attenuation is changed. 90% of the light collected from the laser was used for this long external cavity, the polarization of the light injected back into the laser being set to match that of the emitted light using a fiber polarization controller. The remaining 10% of the light was analyzed using a power-meter and optical and electrical spectrum analyzers.

Similarly, it is not possible to independently control the strength and phase of the optical feedback reflected by the tip of the fiber: a Melles Griot three-axis piezo-micropositioner was used to move the fiber closer to or away from the device, which affected both feedback phase and strength due to the divergence of the beam emitted by the DUT.

Depending on the type of fiber used, the short-cavity feedback can either be enhanced or suppressed: when studying the FP laser, a cleaved fiber was thus used to re-inject about 3% of the light into the cavity. On the contrary, as will be explained in Section V, an AR-coated long-focus lens-ended fiber was used with the TULs in order to minimize any parasitic feedback coming from the fiber and study the effect of long-cavity feedback only.

The lasers are thus studied as follows: a FP laser is first studied under short-cavity feedback in order to assess the sensitivity of the device to such feedback. The results are presented in Section III. Section IV then presents the results obtained when long-cavity feedback is added to the short-cavity one. In order to verify conclusions derived from the behavior of the FP laser, TULs are then studied under long-cavity feedback only, as mentioned above. Section V presents the results obtained, and the effect of long-cavity feedback is discussed.

III. FP Laser Under Short-Cavity Feedback

In this section, the effect of a short-cavity feedback is studied on a FP laser. The external mirror of the cavity is created by the facet of a cleaved fiber placed on a mount holding it with an angle of 10° to the vertical to correspond to the emission angle of the vertical couplers. The shortest achievable distance between the facet of the fiber and that of the laser being of about 10 μm and the piezo-micropositioner having a fine displacement range of 20 μm, the average length of the external cavity is estimated to be of 20 μm. The FP laser is kept at a temperature of 20°C, where its threshold current is 23 mA.

To verify the effect of the fiber position on the laser, measurements of the power collected by the fiber were performed for minute displacements of the fiber along the vertical axis. Fig. 3 presents the coupled power for various voltages applied to the actuator, with the laser biased at 55 mA. The fiber displacement does not appear to linearly follow the applied voltage, as these actuators also exhibit hysteresis, hence the applied voltage will be used in the following graphs in place of the actual distance between the fiber and laser facets. Note that this distance increases as the voltage decreases, thus in Fig. 3 the fiber is the closest to the laser for an applied voltage of 1.5 V.

It can be seen that the overall power tends to drop as the voltage decreases, which corresponds to the loss in coupling resulting from the fiber displacement away from the laser. The graph presents a clear periodicity, which confirms that the fiber position influences the laser output and that a short-cavity feedback is created, its phase changing as the fiber moves. It is however difficult to estimate how the feedback strength is evolving.

Fig. 4 presents the evolution of the optical spectrum of the laser for two slightly different positions of the cleaved fiber. After reaching threshold, emission at a single frequency dominates while all other FP modes are rejected by, e.g., more than 35 dB at 40 mA, as it can be seen in Fig. 4(c). Above 60 mA, dissimilar behaviors are observed for the different positions of the fiber: in Fig. 4(a) the laser emits in a multimode fashion while in Fig. 4(b) the laser remains single-mode but switches to another longitudinal mode. Multi-mode emission is only achieved for currents above 75 mA. In addition, it can be seen in Fig. 4(d) that multi-mode emission does not show a typical gain profile but exhibits a modulation of the spectrum that can be distinguished in both maps. This evolution of the spectrum is very similar to that of recent lasers with an integrated filtered-feedback section [25].

Fourier transforms of below- and above-threshold optical spectra were used to identify the various FSRs of the cavities leading to the observed spectra. Assuming a group index of 4, that of the Si waveguides, the FSR corresponding to the overall modulation of the spectrum would correspond to a cavity

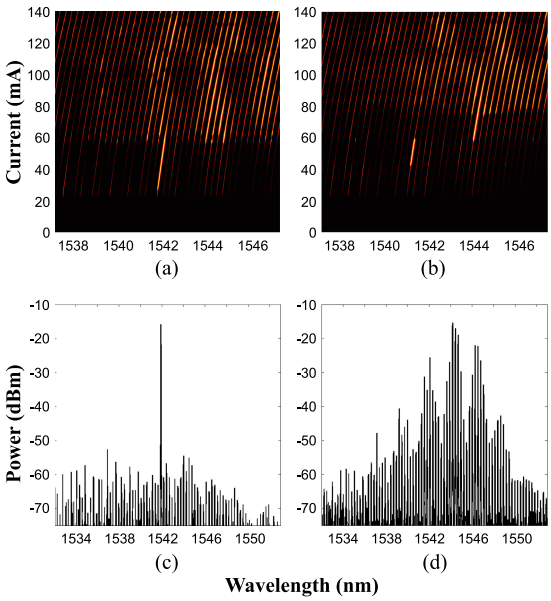

Fig. 4. Top, mappings of the evolution of the optical spectrum of the FP laser for two random positions of the cleaved fiber. Bottom, excerpts from (a) showing spectra at (c) 40 and (d) 80 mA.

between 130 and 150 μm. Unlike a traditional external cavity scheme, where the external reflector creates a cavity that is longer than the laser cavity, a sub-cavity within the laser cavity is observed in this case. Comparing the calculated sub-cavity length with the dimensions of the Si waveguides, the sub-cavity may either stem from reflections between the DBRs and the taper regions, in which case it would be inside the laser cavity, or correspond to the cavity between the fiber facet and the low-reflectivity DBR, which would make it a parasitic cavity outside the laser cavity.

These two cases are in fact similar as they both correspond to a sub-cavity outside the gain region, with most of the cavity within the Si waveguide, and further study of the laser design is necessary to know whether the taper region can indeed generate enough reflections to create such a sub-cavity.

We thus observe that the FP laser shows great sensitivity to short-cavity feedback, revealing in addition that the emission spectrum is strongly affected by a sub-cavity shorter than the laser cavity. As this results in various modal behaviors depending on the position of the fiber, the effect of the short-feedback on the behavior under long-feedback is investigated in Section IV.

IV. FP Laser Under Short- and Long-Cavity Feedback

Fig. 5 presents the evolution of the coupled power depending on the two degrees of freedom corresponding to each cavity, with the laser biased at 55 mA. Here, the short-cavity feedback phase and strength are still controlled by the voltage applied to the piezo-micropositioner, but the long-cavity feedback strength is now controlled by the attenuation of the back-reflector. Note that while moving the fiber also affects the phase of the long-cavity feedback, this has proven to have little effect on the behavior

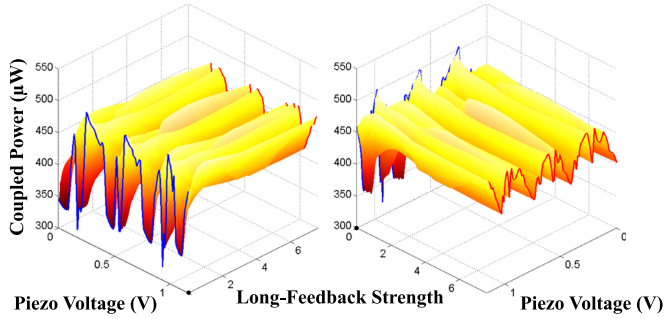

Fig. 5. Evolution of the coupled light with both the voltage applied to the piezoelectric actuator (controlling the short cavity-feedback) and long-feedback strength. The same 3D plot is shown from two angles: one revealing the periodicity of the short-feedback for a long-feedback strength of 0% (blue curve), the other for a long-feedback strength of 7.6% (red curve).

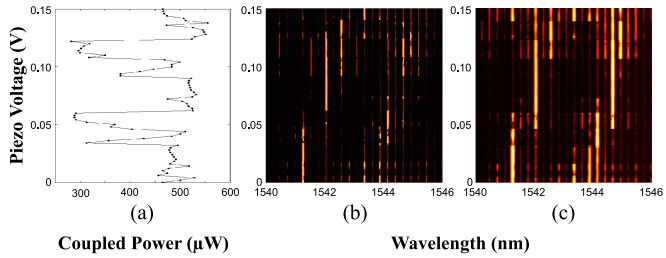

Fig. 6. Evolution with the voltage applied to the piezoelectric actuator of (a) the coupled power, and of the optical spectrum with a long-feedback strength of (b) 0% and (c) 7.6%.

of reference DFB and FP lasers tested in the same setup, and we thus make the assumption that the effect is negligible. The same 3-D plot is shown following two angles in order to observe the evolution of the power with the position of the fiber when the long-feedback strength is minimum (blue line) and maximum (red line).

For a long-feedback strength of 0% (at the minimum feedback level of -64 dB), the blue line reveals the same pattern as that shown in Fig. 3. As the long-feedback strength increases, the FP laser appears to follow different routes depending on the fiber position. Indeed, under maximum long-feedback strength, the red line shows a different pattern than the blue line but with the same periodicity.

Fig. 6 presents the evolution of the optical spectrum corresponding to the variation in coupled power. In Fig. 6(a), the same pattern as in Fig. 3 can be recognized. Fig. 6(b) presents the evolution of the optical spectrum as the fiber is moved, without long-cavity feedback. Drastic changes in the optical spectrum can be observed as the short-feedback parameters change. When the long-cavity feedback is added to the short-cavity one it can be seen that, while the modes broaden, the power distribution does not change and the same modes remain dominant.

The broadening of the modes is characteristic of the apparition of chaotic dynamics. Fig. 7 thus presents electrical spectra measured for three different voltages applied to the micro-positioner, and with three levels of long-feedback strength. The black curves show the RF spectra of the laser without long-cavity feedback.

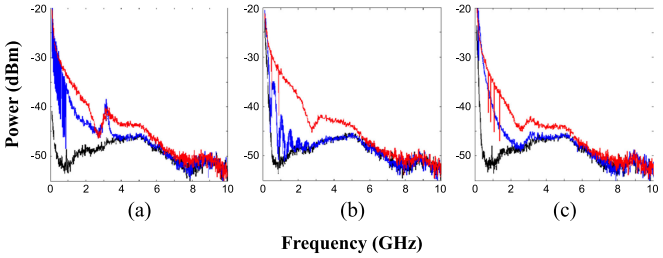

Fig. 7. Evolution of the electrical spectra for the following piezo-micropositioner voltages: (a) 0.03 V, (b) 0.1 V, (c) 0.14 V. The different long-feedback strengths are 0% (black curves), 4% (blue curves) and 7.6% (red curves).

The main differences between these spectra are the low-frequency components, which correspond to partition noise. Fig. 7(a) presents the evolution of the spectra for a voltage of 0.03 V, and it can be seen in Fig. 6(b) that at this voltage one mode dominates hence the modal competition is weak and the partition noise is lower than in the other two cases. The route followed by this mode as the long-feedback strength is increased resembles a traditional route to chaos, where relaxation oscillations undamp and lead to a chaotic regime, which can be identified in the RF spectrum by first the apparition of a peak at the relaxation oscillation frequency of the laser, followed by a strong increase of the spectrum pedestal. However, it can be seen that for the other two fiber positions, different routes to chaos are observed and the chaotic spectra slightly differ. The parasitic effect of the short-cavity feedback thus has a great impact on the behavior of the laser in a long-cavity feedback scheme.

In fact, the modal behavior under long-cavity feedback is dictated by the short-cavity feedback, which acts as a seed. Diverse routes to chaos, each leading to chaotic signals with slightly different spectra, can thus be observed for a given operation point of the FP laser.

V. Tunable Lasers

To conclude this study of hybrid III-V/Si devices under optical feedback, a TUL is studied using only long-cavity feedback. As previously mentioned, these devices were cleaved within the III-V region towards the end of the taper region, allowing us to perform optical feedback experiments by injecting light directly into the active region. It also removed a potential source of reflections as both the low-reflectivity DBR and one of the vertical coupler were cut away. For practical applications, these devices are meant to be biased below 100 mA and the two ring resonators must be tuned to obtain stable single-mode emission. In order to study the devices in unstable regimes, we first biased the device at 100 mA and tuned the resonators to obtain single-mode emission, then mapped the optical and electrical spectra of the free-running TUL for bias currents up to 200 mA.

Fig. 8 presents the evolution of the optical and electrical spectra as the bias current is increased. The optical spectra show that, as the laser red-shifts and is detuned from the ring resonators, it enters regions of bi-modal emission. Fig. 8(b) shows that

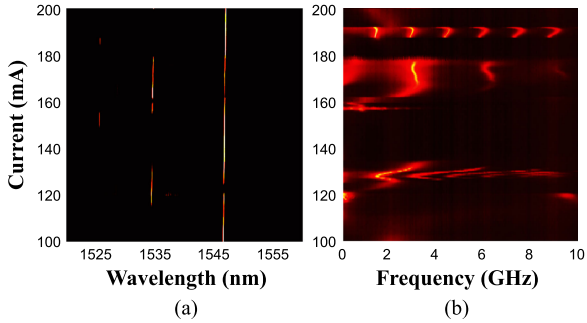

Fig. 8. Mapping of the (a) optical and (b) electrical spectrum of the free-running TUL as a function of the bias current.

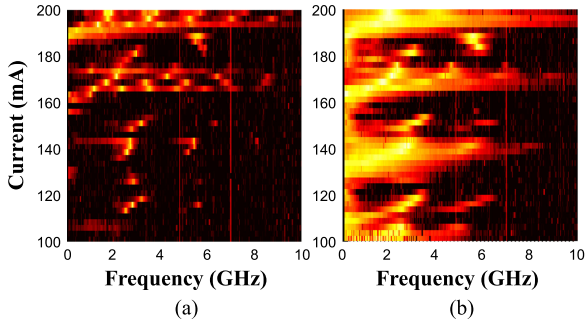

Fig. 9. Mapping of the electrical spectrum of the TUL with bias current (a) in free-running operation and (b) under long-cavity feedback with a 7.5% strength. The two vertical red lines are measurement artifacts stemming from the RF spectra processing.

these regions of bi-modal emission correspond to regions of oscillations. While these oscillations resemble exalted relaxation oscillations with harmonics, the evolution of the main oscillation frequency does not evolve in the expected manner as the bias current increases.

Around 190 mA, the single-mode laser enters a region of strong periodic oscillations. Unlike the FP laser studied previously, the TUL is here in free-running operation: a long-focus anti-reflection-coated lens-ended fiber is used to collect the light emitted by the laser, thus suppressing any short-cavity feedback that could be created by the tip of the fiber, and the laser is not yet subjected to long-cavity feedback. This was indeed verified by repeating measurements for various positions of the fiber, which this time had no effect on the dynamics of the laser. Any source of instability may thus come from the laser cavity itself as the Si section of the TUL consists of several Si waveguide including the ring resonators.

Finally, Fig. 9 presents the evolution of the electrical spectra of the TUL with its bias current in free-running operation and under strong long-cavity feedback. The two maps look very similar and reveal that instead of following a route to chaos for all currents, the laser only seems to take a route towards a chaotic regime from its free-running dynamics. Around 120 mA, where the free-running laser is stable, the laser does not exhibit chaotic dynamics under strong long-cavity feedback and only low-frequency components can be observed.

Without being subjected to an additional short-cavity feedback, the overall behavior of the TUL is very similar to that of the FP laser. While the FP laser was destabilized intentionally using a short-cavity feedback, the TUL appears to suffer from instabilities that could stem from sub-cavities within the laser cavity since no external cavity short-cavity is created in this case. In a similar fashion to the modal behavior of the FP laser, the dynamic behavior of the TUL under long-cavity feedback builds upon the instabilities caused by these sub-cavities.

VI. Conclusion

Both lasers studied showed great sensitivity to external optical feedback. In the FP laser, this sensitivity translates into complex modal behaviors. If the FP laser were to be used in a PIC, any component reflecting light towards it within the microchip would thus greatly affect its operation. Modal competition being suppressed in the TUL, this instability appeared as strong periodic oscillations of the total output power of the laser. The lasers are affected by sub-cavities in the Si waveguides, which are however difficult to identify without being able to characterize individually the sections of the laser corresponding to a transition from one waveguide to another. Nevertheless, both scenarios show that the combination of complicated laser design with external perturbations indeed leads to complex behaviors.

These results are of prime importance for the development of future laser sources for integrated photonics applications. Feedback sources in Si waveguides must be identified and controlled, as the laser cannot be protected from those using external isolators. Applications requiring the use of optical feedback must also ensure that the laser dynamics under feedback are predictable and do not depend on a sub-cavity.

Future experimental work will concentrate on the study of III-V/Si lasers in several realistic feedback schemes, with cavities of a few centimeters (typ. around 5 cm). These intermediate cavity lengths would closely match that of the parasitic feedback cavities usually found in PICs, which would allow evaluating the behavior of various designs of III-V/Si laser sources under a realistic multiple-cavity configuration. With external cavities of similar lengths, the impact of such multiple cavities may indeed be very different from what is observed in this work, where the smallest one dominates the overall dynamics.

The study of the dynamics of DFB lasers under long-cavity feedback will also allow comparison of the behavior of hybrid III-V/Si lasers with well-known quantum well and quantum dot III-V laser sources. In addition, a theoretical study of a DFB laser subjected to several feedback sources with different external cavity lengths would be necessary to fully understand the effect of such combinations of feedback for Si lasers. Using the Lang-Kobayashi laser equation in the context of multiple feedback sources with parameters and cavity lengths specific to III-V/Si lasers should yield interesting results. Using rate equations may however not allow fully accounting for the complex interaction between modes in-between the two taper regions of the devices presented in this study, which may require travelling-wave modeling of a simplified design.

References

[1] L. Vivien and L. Pavesi, *Handbook of Silicon Photonics*. New York, NY, USA: Taylor & Francis, 2014.

[2] C. Sun *et al.*, "Single-chip microprocessor that communicates directly using light," *Nature*, vol. 528, pp. 534–538, 2015.

[3] M. Asghari and A. V. Krishnamoorthy, "Silicon photonics: Energy-efficient communication," *Nature Photon.*, vol. 5, pp. 268–270, 2011.

[4] A. Rickman, "The commercialization of silicon photonics," *Nature Photon.*, vol. 8, pp. 579–582, 2014.

[5] P. Chaisakul *et al.*, "Integrated germanium optical interconnects on silicon substrates," *Nature Photon.*, vol. 8, pp. 482–488, 2014.

[6] P. Dong, Y.-K. Chen, G.-H. Duan, and D. T. Neilson, "Silicon photonic devices and integrated circuits," *Nanophotonics*, vol. 3, pp. 215–228, 2014.

[7] L. Virot *et al.*, "Germanium avalanche receiver for low power interconnects," *Nature Commun.*, vol. 5, pp. 49–57, 2014.

[8] G. T. Reed, G. Mashanovich, F. Gardes, and D. Thomson, "Silicon optical modulators," *Nature Photon.*, vol. 4, pp. 518–526, 2010.

[9] D. Liang and J. E. Bowers, "Recent progress in lasers on silicons," *Nature Photon.*, vol. 4, pp. 511–517, 2010.

[10] G.-H. Duan *et al.*, "Hybrid III–V on silicon lasers for photonic integrated circuits on silicon," *IEEE J. Sel. Topics Quantum Electron.*, vol. 20, no. 4, Jul./Aug. 2014, Art. no. 6100213.

[11] C. Wang, X.-L. Zhong, and Z.-Y. Li, "Linear and passive silicon optical isolator," *Sci. Rep.*, vol. 2, 2012, Art. no. 674.

[12] M. Vanwolleghem *et al.*, "First experimental demonstration of a monolithically integrated InP-based waveguide isolator," in *Proc. Opt. Fiber Commun. Conf.*, Los Angeles, CA, USA, 2004, p. 401.

[13] W. Van Parys *et al.*, "Study of a magnetooptic contact for an amplifying waveguide optical isolator," *IEEE Photon. Technol. Lett.*, vol. 19, no. 9, pp. 659–661, May 2007.

[14] R. E. Camacho-Aguilera *et al.*, "An electrically pumped germanium laser," *Opt. Express*. vol. 20, pp. 11316–11320, 2012.

[15] A. Lee, Q. Jiang, M. Tang, A. Seeds, and H. Liu, "Continuous-wave InAs/GaAs quantum-dot laser diodes monolithically grown on Si substrate with low threshold current densities," *Opt. Express*, vol. 20, pp. 22181–22187, 2012.

[16] A. Y. Liu *et al.*, "High performance continuous wave 1.3 μm quantum dot lasers on silicon," *Appl. Phys. Lett.*, vol. 104, 2014, Art. no. 041104.

[17] G. Roelkens *et al.*, "III-V/Si photonics by die-to-wafer bonding," *Mater. Today*, vol. 10, nos. 7/8, pp. 36–43, 2007.

[18] H. Park *et al.*, "Device and integration technology for silicon photonic transmitters," *IEEE J. Sel. Topics Quantum Electron.*, vol. 17, no. 3, pp. 671–688, May/Jun. 2011.

[19] J. C. Hulme, J. K. Doylend, and J. E. Bowers, "Widely tunable Vernier ring laser on hybrid silicon," *Opt. Express*, vol. 21, pp. 19718–19722, 2013.

[20] F. Grillot, G. H. Duan, and B. Thedrez, "Feedback sensitivity and coherence collapse threshold of semiconductor DFB lasers with complex structures," *IEEE J. Quantum Electron.*, vol. 40, no. 3, pp. 1–11, Mar. 2004.

[21] R. W. Tkach and A. R. Chraplyvy, "Regimes of feedback effects in 1.5-μm distributed feedback lasers," *J. Lightw. Technol.*, vol. LT-4, no. 1, pp. 1655–1661, Nov. 1986.

[22] F. Grillot, B. Thedrez, V. Voiriot, and J. L. Lafragette, "Coherence collapse threshold of 1.3μm semiconductor DFB lasers," *IEEE Photon. Technol. Lett.*, vol. 15, no. 1, pp. 9–11, Jan. 2003.

[23] G. Kurczveil, P. Pintus, M. J. R. Heck, J. D. Peters, and J. E. Bowers, "Characterization of insertion loss and back reflection in passive hybrid silicon tapers," *IEEE Photon. J.*, vol. 5, no. 2, 2013, Art. no. 6600410.

[24] A. Argyris, M. Hamacher, K. E. Chlouverakis, A. Bogris, and D. Syvridis, "Photonic integrated device for chaos applications in communications," *Phys. Rev. Lett.*, vol. 100, no. 19, pp. 194101–194104, 2008.

[25] J. Zhao *et al.*, "Stability of a monolithic integrated filtered- feedback laser," *Opt. Express*, vol. 20, pp. 270–278, 2012.

[26] D. D'Agostino, D. Lenstra, H. P. M. M. Ambrosius, and M. K. Smit, "Coupled cavity laser based on anti-resonant imaging via multimode interference," *Opt. Lett.*, vol. 40, pp. 653–656, 2015.

[27] A. Karsaklian Dal Bosco *et al.*, "Cycles of self-pulsations in a photonic integrated circuit," *Phys. Rev. E*, vol. 92, 2015, Art. no. 062905.

[28] S. Chen *et al.*, "Electrically pumped continuous-wave III–V quantum dot lasers on silicon," *Nature Photon.*, vol. 10, pp. 307–311, 2016.

Kevin Schires received the Diplôme d'Ingénieur degree, specializing in signal processing and telecommunications, from the École Supérieure d'Ingénieurs en Électronique et Électrotechnique, Paris, France, and the Ph.D. degree in semiconductor electronics from the University of Essex, Colchester, U.K. He is currently holding a Postdoctoral Position in the Communications and Electronic Department, Telecom Paristech (alias Ecole Nationale Supérieure des Télécommunications) focused on the study of the dynamics of novel semiconductor laser sources under optical injection and optical feedback.

Nils Girard received the Master's degree of engineering (option: photonics) from SUPELEC, Gif-sur-Yvette, France, and the Master's of Science (physics, plasma, photonics) degree from the University of Metz-Nancy, Metz, France, in 2012. Since November 2012, he has been working toward the Ph.D. degree with the III–V Lab, Palaiseau, France, to work on low-noise hybrid III–V/silicon lasers for radar and ultrastable clocks applications. Later this year, he worked with Thales Research and Technology on the generation of RF signal with dualfrequency VECSEL.

Ghaya Baili was born in Tunisia in 1980. She received the Master's degree in optics and photonics from the Ecole Superieure d'Optique, University of Paris XI, Orsay, France, in 2004, where she also received the Ph.D. degree in laser physics, in 2008. She joined Thales Research & Technology, Palaiseau, France, in 2005. Her research interests include noise reduction in continuous, dualfrequency, and mode-locked semiconductor lasers for microwave photonics applications. She is the Member of the Societe Francaise d'Optique.

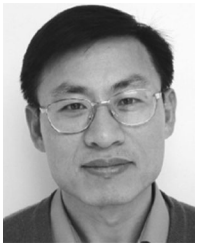

Guang-Hua Duan (S'88–M'90–SM'01) received the Doctorate degree in 1991 from the Ecole Nationale Supérieure des Télécommunications (Telecom-ParisTech), Paris, France, in applied physics. He was habilitated to direct researches by Université de Paris-Sud in 1995. He is currently the Leader of the research team "Silicon Photonics" within III-V Lab, which is a joint laboratory of Nokia, Thales, and CEA Leti. He is also a Guest Professor in Ecole Supérieure d'Elecricité, Gif-sur-Yvette, France, and Ecole Supérieure d'Optique, Palaiseau, France, giving lectures in the fields of electromagnetism, optoelectronics, and laser physics. Previously, he had been an Assistant, then an Associate Professor at Telecom-ParisTech from 1992 to 2000. He was with the University of Maryland as a Visiting Associate Professor from 1998 to 1999. He joined Opto+, Alcatel Research & Innovation Center in Marcoussis on October 2000. He is author or co-author of more than 100 journal papers, 250 conference papers, 30 patents and a contributor to four book chapters.

Sandra Gomez received the Bachelor's and Master's degrees in electrical engineering from the Stevens Institute of Technology, Hoboken, NJ, USA, with a concentration in digital signal processing. She joined the Ph.D. degree at TELECOM Paris Tech in September 2015. She is the Technical Director of the International Technology Center, France, part of the US Army Research, Development, and Engineering Command (RDECOM) Forward Element Center Atlantic located in Paris, France. She previously studied acoustic source localization and the tradeoffs of conventional and adaptive beamforming techniques using different uniform circular array configurations to differentiate between interfering signals and a particular signal of interest. Her thesis is focused on advanced laser diodes using new materials in particular those with III-V on silicon, nonlinear dynamics and optical chaos in semiconductor laser systems.

Previously, she worked at the US Army RDECOM Armament Research, Development, and Engineering Center where she served as a Project Officer in the Acoustic and Networked Sensor Division with specific program responsibility in the development of advanced acoustic sensors. She has a strong foundation in systems engineering and extensive experience in defense acquisition, program management, and Life Cycle Support.

Frédéric Grillot was born in Versailles, France, on August 22, 1974. He received the M.Sc. degree from the University of Dijon, Dijon, France, 1999, and the Ph.D. degree from the University of Besançon, Besançon, France, in 2003. His doctoral research activities were conducted within the optical component research department in Alcatel-Lucent working on the effects of the optical feedback in semiconductor lasers, and the impact this phenomenon has on optical communication systems. From 2003 to 2004, he was with the Institut d'Electronique Fondamentale (University Paris-Sud) where he focused on integrated optics modeling and on Si-based passive devices for optical interconnects. From September 2004 to September 2012, he was working with the Institut National des Sciences Appliquées as an Assistant Professor. From 2008 to 2009, he was also a Visiting Professor at the University of New-Mexico, Albuquerque, NM, USA, leading research in optoelectronics at the Center for High Technology Materials. Since October 2012, he has been appointed as an Associate Professor within the Communications and Electronic Department, Telecom Paristech (alias Ecole Nationale Supérieure des Télécommunications), Paris, France. Since August 2015, he has been serving as a Research Professor at the University of New-Mexico. He is the author or coauthor of 70 journal papers, one book, two book chapters, and more than 150 contributions in international conferences and workshops. His current research interests include advanced laser diodes using new materials including quantum dots and dashes for low-cost applications, nonlinear dynamics and optical chaos in semiconductor lasers systems as well as microwave and silicon photonics applications including photonic clocks and photonic analog to digital converters. He is an Associate Editor for *Optics Express*, Senior Member of the SPIE and of the IEEE Photonics Society, as well as a Member of the OSA